ANNALS OF GEOPHYSICS, 67, 5, SA549, doi:10.4401/ag-9107
OPEN ACCESS

Induced geoelectric field: influence of polarization in coast effect and proximity effect

Giovanni Lucca*,[1]

(1) Retired Independent Researcher

Article history: received May 3, 2024; accepted September 25, 2024

Abstract

During a magnetic storm, the induced geoelectric field drives induced currents that couple with artificial metallic networks such as power lines, pipelines, telecommunication cables and railway lines with the consequent risk, in case of strong events, of possible blackouts, damages and impairments of those systems.

It is known that magnetic storms are global phenomena and their effects in specific regions with specific ground conductivity may be different; in particular, when a magnetic storm involves regions composed of two adjacent media characterized by very large difference of conductivity between them (e. g. sea and land) the induced geoelectric field is largely influenced by this conductivity contrast and depends, primarily, on its orientation with respect to the discontinuity line.

By representing the source as an incident plane wave normally directed with respect to the air-land/sea interface, two kinds of polarizations are usually considered in literature: H/E polarization i.e. with the incident magnetic/electric field parallel to the discontinuity.

In this paper, we wish to study a more general case i.e. when the source is characterized by an electric field forming a generic angle with the discontinuity line so that the resulting field is a combination of both H and E polarizations; to do this, and by adopting a 2D approach based on the generalized thin sheet model, the paper combines, published formulas for H polarization while new approximated analytic formulas for E polarization are derived.

Moreover, we express the induced geoelectric field as a function of a generic direction which represents the layout orientation of a potentially affected plant (power line, pipeline...); this is important, because that is the first step necessary to evaluate the level of geomagnetically induced currents (GIC) in the plant itself.

In conclusion, the novelty of this approach is that the resulting induced geoelectric field on the Earth's surface can be expressed using only analytical formulas; a further advantage of the proposed approach to the problem is that it is quite simple and particularly suitable for the evaluation of GIC in terrestrial conductor networks.

Keywords: Geoelectric field; Geomagnetically Induced Currents; Coast effect; Proximity effect; Magnetic storms

1. Introduction

It is known that Geomagnetically Induced Currents (GIC) are the result, at earth surface, of Space Weather which is driven by the activity of the Sun; different kind of plants such as power lines, pipelines, telecommunication cables, railway circuits may be negatively influenced by them (Boteler, 2001a; Boteler, 2001b; Boteler, 2003, Pilipenko, 2021). In fact, consequence of a strong solar activity, is a magnetic storm during which temporal variations of the geomagnetic field induce an electric field at the earth surface; the electromagnetic coupling of such electric field with the above-mentioned technological infrastructures is the cause of GIC. Thus, the first step for assessing GIC inside a system is to evaluate the geoelectric induced field in the region where the influenced system is located.

A common approximation concerning the geoelectric field assessment and regarding the earth conductivity is that the latter one depends only on depth so that the earth can be described by a 1D model; nevertheless, this approximation is not adequate when the affected system is located in an area characterized by large variations of conductivity also in the horizontal direction and, consequently, the earth structure must be described by 2D or 3D models. Typical example is the conductivity contrast at the land-sea interface where the seawater conductivity is much greater than that of the land.

As remarked by previous studies (Fisher, 1979; Gilbert, 2005), it is just the conductivity contrast between sea and land which is responsible for large enhancement of the geoelectric field perpendicular to the coast line. This phenomenon is usually known as the *geoelectric coast effect*.

In certain cases, the conductivity depends only on one of the two horizontal coordinates so that a 2D model may be enough for the purpose of GIC assessment. That may be the case of a long uniform and rectilinear coast (Weaver, 1994).

Different approaches have been proposed in literature, both analytical and numerical, to deal with this problem.

Among the analytical models, it is worth noting the one consisting in a vertical fault of finite depth, above a semi-infinite homogeneous substratum, having zero or infinite conductivity (d'Erceville and Kunetz, 1962), the one of the dike (Rankin, 1962) and the one of the infinite vertical fault (Weaver, 1963). Further details about these models can be found also in (Blake,1968).

These approaches have the limitation of being too idealistic essentially for what concerns the modelling of the substratum (which is supposed having zero or infinite conductivity) or in modelling the sea having infinite depth.

The numerical methods allow to overcome the limitation related to the analytical methods so one can consider earth models characterized by many layers having different values of conductivity; see (Pokhrel, 2018) that proposed a Finite Difference Time Domain (FDTD) approach or (Dong et al., 2015a, Dong et al., 2015b) that adopted a Galerkin Finite Element Method (FEM) model.

Liu et al., (2018), by applying a FEM model, assessed the risk due to GIC for the nuclear power station at Ling'ao in the Guandong Province, located in the coastal region of China.

Liu et al. (2019b; 2019a) studied in two separate works, by FEM models, the effect of H polarization (that is the source magnetic field parallel to the coast) causing the above-mentioned coast effect and of E polarization (that is the source electric field parallel to the coast) causing the so-called *proximity effect*. The latter effect consists in a gradual change of the geoelectric field in the two adjacent areas separated by the discontinuity represented by the coast; such an effect depends (as in the case of H polarization) on the distance from the coast itself. Thus, if a power line or a pipeline is parallel and sufficiently close to the shoreline, the proximity effect can have a significant effect on GIC assessment.

Another different kind of approach to the problem is the thin sheet model. It consists in a simple analytical method that, albeit approximated, allows to overcome many of the difficulties related to the previous mentioned analytical methods; such a model, was first introduced by Price (1949) and its application was reviewed by Ashour (1973) and a generalized thin sheet model was introduced by Ranganayaki and Madden (1980). In fact, while the first thin sheet models can be considered "one-layer model" because they took into consideration only the first conductive layer (sedimentary rock or seawater), Ranganayaki and Madden took into account also of the resistive underlying crustal layer and, from this point of view, their approach can be considered a "two-layer model".

In the PRCI Report (2002), this model is proposed as a successful method for investigating the geoelectric field near a coastline and the basic equations in 2D problems, under H polarization, are given. The same equations have been used by Wang et al. (2023) to construct a very useful analogy between generalized thin sheet model and transmission lines theory.

Nevertheless, it is necessary to add that both the above-mentioned works are limited to the case of H polarization and do not consider the case of E polarization.

Therefore, the first purpose of our work is to propose, under the hypothesis of applicability of a 2D generalized thin sheet model, formulas for the evaluation of the geoelectric field in the case of E polarization.

We also would like to point out that an incident wave which is only H or E polarized represents only the two limiting cases but, a more realistic approach, should consider a source which is a combination of the two polarization modes; so, the second purpose of this paper is to present formulas for the evaluation of the geoelectric field under the hypothesis that the source is a linear combination of H and E polarized modes.

As the study of the geoelectric field is aimed at the assessment of GIC in technological infrastructures, the third purpose of this paper is to propose specific formulas for the geoelectric field that take into account the direction and orientation of the affected infrastructures.

2. Basic hypotheses relevant to the generalized thin sheet model

In this section we present the principal hypotheses on which the 2D generalized thin sheet model of Ranganayaki and Madden (1980) is based.

The drawing in Fig. 1 is useful to introduce the main characteristics and parameters characterizing the model.

Figure 1 represents a section of a long coast having uniform characteristics along the x axis which is supposed entering the sheet so that it represents the line of discontinuity between land and sea; as mentioned in the previous section, the uniformity along the x axis justifies the 2D assumption; thus, the electromagnetic field depends only on y and z coordinates.

According to a simple representation of the Earth conductivity structure, we have a first conductive layer, composed by sedimentary rocks or seawater, below which we find the more resistive Earth's crust and, under that, a more conductive stratified common basement representing the Earth's mantle. Nevertheless, it should be pointed

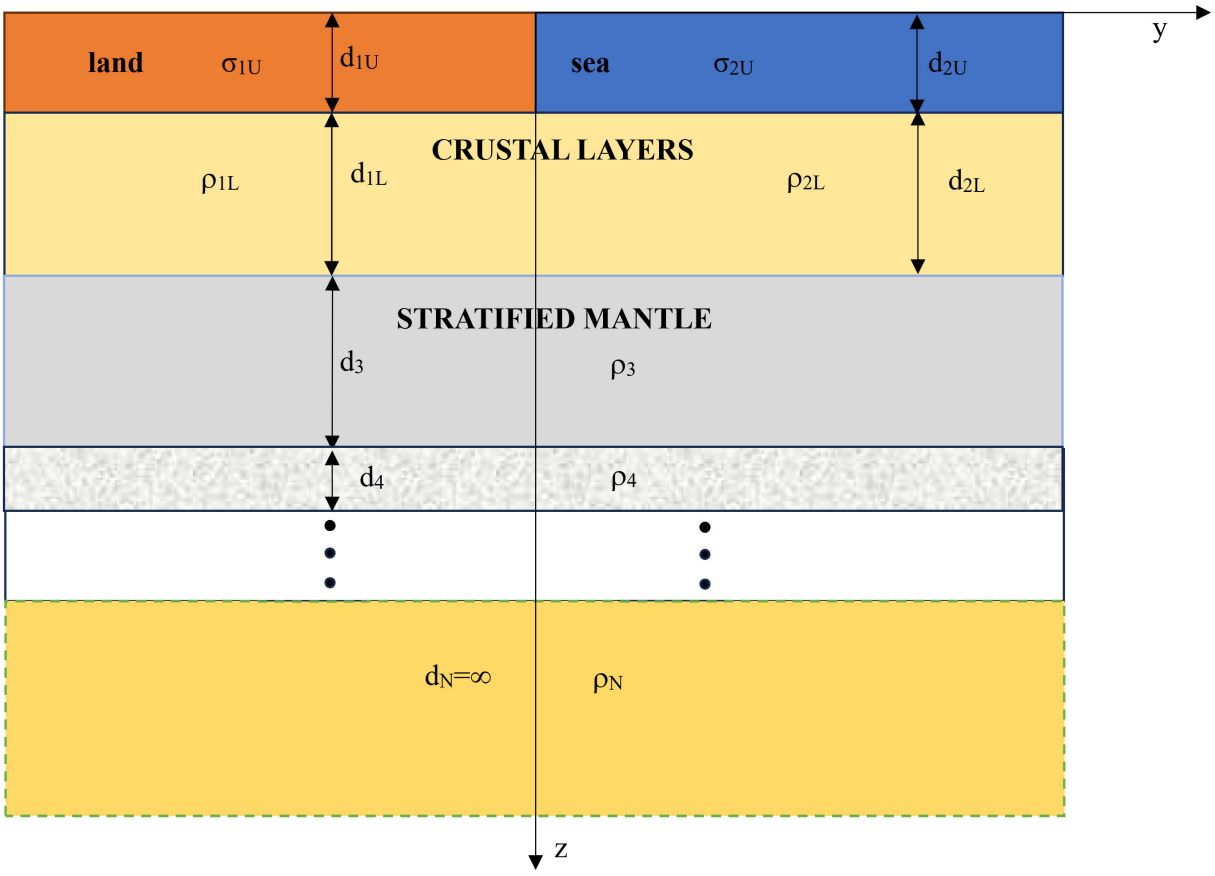

Figure 1. Model of Earth stratification in proximity of a coastline; the first conductive layer is generally composed by sediments (on the left) and seawater (on the right) below which is the resistive crust and under that the Earth's mantle.

out that the model does not strictly request that the basement structure is common to both sides as represented in Fig. 1; in principle, the modelling allows for different basement structures in the two regions (see also Appendix B). Anyway, the model is often presented as in Fig. 1 and represents a reasonable assumption in many cases.

With reference to Fig. 1, σ_{iU} and d_{iU} ($i = 1,2$) represent the conductivity and the thickness of the first (Upper) layer on the land side and sea side respectively; analogously, ρ_{iL} and d_{iL} ($i = 1,2$) represent the resistivity and the thickness of the second (Lower) layer. Finally, if the mantle is composed by N-2 layers (the last one of infinite depth), ρ_i and d_i ($i = 3, 4,..N$) are their resistivity and depth respectively.

The basic physical hypothesis in order that the generalized thin sheet method can be applied is that the electromagnetic fields penetrate through both the first two layers. More specifically, the electric field does not change substantially with depth across the upper layer while the magnetic does not change substantially with depth across the lower layer. Consequently, the thicknesses of these layers must be small compared to the skin depth in those layers (Wang et al., 2023); therefore, in the range of frequencies typically involved in the phenomenon of geoelectric induction (i.e. 0.1 mHz-10 mHz) it must be:

$$\delta_{iU} = \frac{1}{\sqrt{\pi \sigma_{iU} f \mu_0}} \ll d_{iU} \quad i = 1,2 \tag{1a}$$

$$\delta_{iL} = \sqrt{\frac{\rho_{iL}}{\pi f \mu_0}} \ll d_{iL} \quad i = 1,2 \tag{1b}$$

With f the frequency, μ_0 the vacuum magnetic permeability and δ_{iU} and δ_{iL} ($i = 1,2$) the skin depth in the media relevant to the first and second layer respectively.

Then, inequalities (1) imply restrictions on the frequencies and layer thicknesses for which this method can be used; nevertheless, the above-mentioned interval (0.1 mHz-10 mHz) practically covers most of range of frequencies involved in geomagnetic disturbances on ground infrastructures.

3. Formulas for H and E polarization

3.1 General assumptions

We report here, for convenience, the formulas for the geoelectric field as a function of the distance from the coast y and of the frequency f evaluated for $z = 0$ that is at the surface of the land and sea. We give the expressions for the cases of H and E polarization.

The geoelectric field is expressed in phasor form by supposing a time dependency of the type $exp(j\omega t)$ with j the imaginary unit and $\omega = 2\pi f$ the angular frequency.

The source of the electromagnetic field is represented by a uniform plane wave vertically incident on the Earth's surface represented by the xy plane, and polarized as shown in Fig. 2; E, H are the electric, magnetic fields respectively while S is the Poynting vector.

In the following, we present in separate subsections the formulas for the geoelectric field in the cases of H and E polarizations.

We also add that those formulas can be generalized to the case of more than two adjacent media with different conductivities. An example with three media is presented in Appendix B.

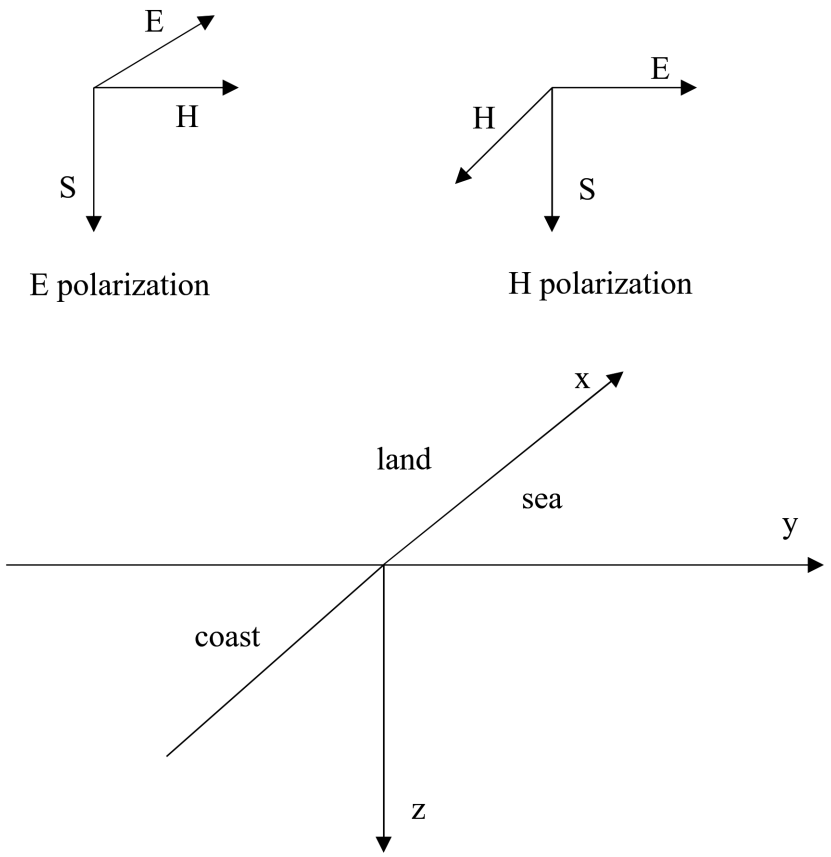

Figure 2. Scheme of E and H polarization; on the top left and top right it is represented a uniform plane wave vertically incident on the Earth's surface in case of E polarization and H polarization respectively.

3.2 H polarization

For the case of H polarization, according to Ranganayaki and Madden (1980) (but see also PRCI Report (2002) and Wang et al. (2023), one has:

$$E_y(y,f) = \begin{cases} \dfrac{\tau_2 E_2^0(f) - \tau_1 E_1^0(f)}{\sqrt{\tau_1\lambda_1}\left(\dfrac{\tau_1}{\sqrt{\tau_1\lambda_1}} + \dfrac{\tau_2}{\sqrt{\tau_2\lambda_2}}\right)} e^{\frac{y}{\sqrt{\tau_1\lambda_1}}} + E_1^0(f) & y < 0 \\ \dfrac{\tau_2 E_2^0(f) - \tau_1 E_1^0(f)}{\sqrt{\tau_2\lambda_2}\left(\dfrac{\tau_1}{\sqrt{\tau_1\lambda_1}} + \dfrac{\tau_2}{\sqrt{\tau_2\lambda_2}}\right)} e^{\frac{-y}{\sqrt{\tau_2\lambda_2}}} + E_2^0(f) & y > 0 \end{cases} \tag{2}$$

In formula (2), the quantities $E_1^0(f)$ and $E_2^0(f)$ represent the incident electric field at large distance from the coast so that the effect of the discontinuity is negligible while $\tau_i = \sigma_{iU}.d_{iU}$ and $\lambda_i = \rho_{iL}.d_{iL}.(i = 1,2)$. If H^0 is the incident magnetic field supposed constant all over the area under study, $E_1^0(f)$ and $E_2^0(f)$ are related to it by means of the relation:

$$E_i^0(f) = -Z_{Ti}(f)H^0 \quad i = 1,2 \tag{3}$$

In formula (3), Z_{Ti} is the surface impedance relevant to the stratified medium (land or sea) evaluated very far from the discontinuity so that its effect can be considered negligible.

For the following, by means of Eq. (3), it is convenient to rewrite Eq. (2) as follows:

$$E_y(y,f) = \begin{cases} \dfrac{[-\tau_2 Z_{T2}(f) + \tau_1 Z_{T1}(f)]H_0}{\sqrt{\tau_1\lambda_1}\left(\dfrac{\tau_1}{\sqrt{\tau_1\lambda_1}} + \dfrac{\tau_2}{\sqrt{\tau_2\lambda_2}}\right)} e^{\frac{y}{\sqrt{\tau_1\lambda_1}}} - Z_{T1}(f)H_0 & y < 0 \\ \dfrac{[-\tau_2 Z_{T2}(f) + \tau_1 Z_{T1}(f)]H_0}{\sqrt{\tau_2\lambda_2}\left(\dfrac{\tau_1}{\sqrt{\tau_1\lambda_1}} + \dfrac{\tau_2}{\sqrt{\tau_2\lambda_2}}\right)} e^{\frac{-y}{\sqrt{\tau_2\lambda_2}}} - Z_{T2}(f)H_0 & y > 0 \end{cases} \tag{4}$$

Explicit formulas for calculating the surface impedance Z_{Ti}, by means of a recursive relation, are given by Trichtchenko and Boteler (2002).

3.3 E polarization

For the case of E polarization, we need to define the following quantities:

$$K_i(f) = \frac{j\omega\mu_0 d_{Li} + Z_{Ti\_3}(f)}{1 + \sigma_{iU} d_{iU}\left[j\omega\mu_0 d_{Li} + Z_{Ti\_3}(f)\right]} \quad i = 1,2 \tag{5}$$

$$\Gamma_i(f) = \sqrt{\frac{j\omega\mu_0}{d_{iU} K_i(f)}} \quad i = 1,2 \tag{6}$$

$Z_{Ti\_3}(f)$ is the surface impedance of the i-th medium "seen" from the interface between the second and the third layer (i.e. the common basement representing the mantle shown in Fig. 1).

The formulas for the electric field are:

$$E_x(y,f) = \begin{cases} \dfrac{H_0[K_2(f) - K_1(f)]\Gamma_2(f)}{\Gamma_2(f) + \Gamma_1(f)} e^{\Gamma_1(f)y} + H^0 K_1(f) & y < 0 \\ \dfrac{-H_0[K_2(f) - K_1(f)]\Gamma_1(f)}{\Gamma_2(f) + \Gamma_1(f)} e^{-\Gamma_2(f)y} + H^0 K_2(f) & y > 0 \end{cases} \tag{7}$$

See Appendix A for the deduction of the formulas in the E polarization case and the main simplifying assumptions on which they are based.

Notice that in case of H polarization the induced geoelectric field is directed along the y-axis (i.e. perpendicular to the discontinuity) while, in the case of E polarization, it is directed along the x-axis (i.e. parallel to the discontinuity).

4. Case of generic polarization and induced emf

The previous formulas are valid in two limit cases:

- The incident magnetic field is parallel to the discontinuity (H polarization).
- The incident electric field is parallel to the discontinuity (E polarization).

Here we want to consider the more general case of a plane wave (normally incident to the air-land/sea interface) that is expressed as a linear combination of the H and E polarization modes.

Firstly, it is convenient to define a polarization angle ψ as the angle between the x-axis i.e. the line of conductivity discontinuity and the direction of the incident electric field (see Fig. 3).

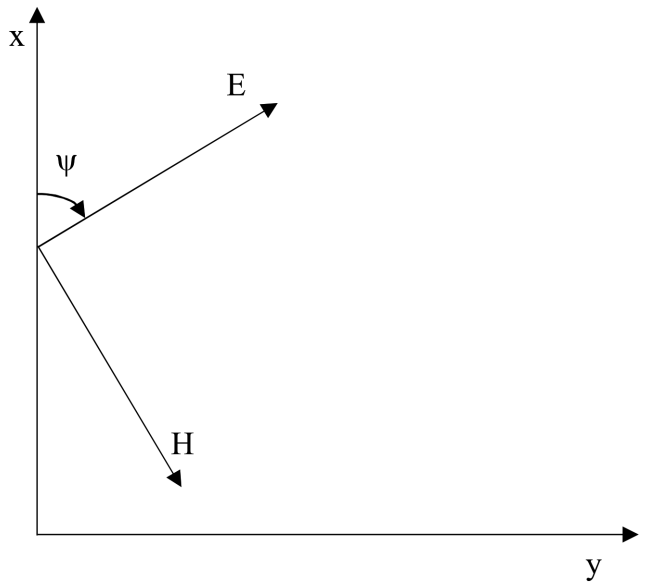

Figure 3. Definition of the polarization angle ψ; the x-axis represents the coastline while E and H are the vertically incident electric and magnetic fields on the Earth's surface represented by the xy plane. For $\psi = 0°$ or $\psi = 180°$ one has pure E polarization while for $\psi = 90°$ or $\psi = 270°$ pure H polarization.

Therefore, the total electric field $\vec{E}(y, f)$ combination of the two modes of polarization is given by:

$$\vec{E}(y, f, \psi) = E_x(y, f)(\cos\psi)\vec{u}_x + E_y(y, f)(-\sin\psi)\vec{u}_y \tag{8}$$

Where $\vec{u}_x$ and $\vec{u}_y$ are the unit vectors relevant to x and y axes respectively.

This formula is intended for the evaluation of GIC in technological system which, in many cases, are represented by long straight conductors (power lines, pipelines, telecommunication cables); these conductors together with the ground form a circuit where the GIC are driven by the induced emf (electromotive force) generated in the circuit itself by the time varying geomagnetic field.

Boteler (1999) has shown that the above mentioned emf e can be calculated as the integral of the induced geoelectric field along the path Γ (that represents the layout of the influenced technological system) that is:

$$e = \int_{\Gamma} \vec{E} \cdot d\vec{\Gamma} \tag{9}$$

As the total induced emf e depends not only on the amplitude and direction of the geoelectric field but also on the path Γ, it is important to consider also the direction and the geometry of the latter.

If we consider an infinitesimal element of the path $d\Gamma$, from Eq. (9) we have:

$$de = \vec{E} \cdot d\vec{\Gamma} \tag{10}$$

Where $\vec{E}$, according to Eq. (8) depends on the polarization angle ψ, while $d\vec{\Gamma}$ depends on the angle θ formed between the direction of $d\vec{\Gamma}$ and the x axis as shown in Fig. 4.

Thus, the angle θ is related to the orientation of the influenced technological system with respect to the coastline and, in most of cases, this angle is variable along the system layout; in the following, we shall briefly denote it by *orientation angle*.

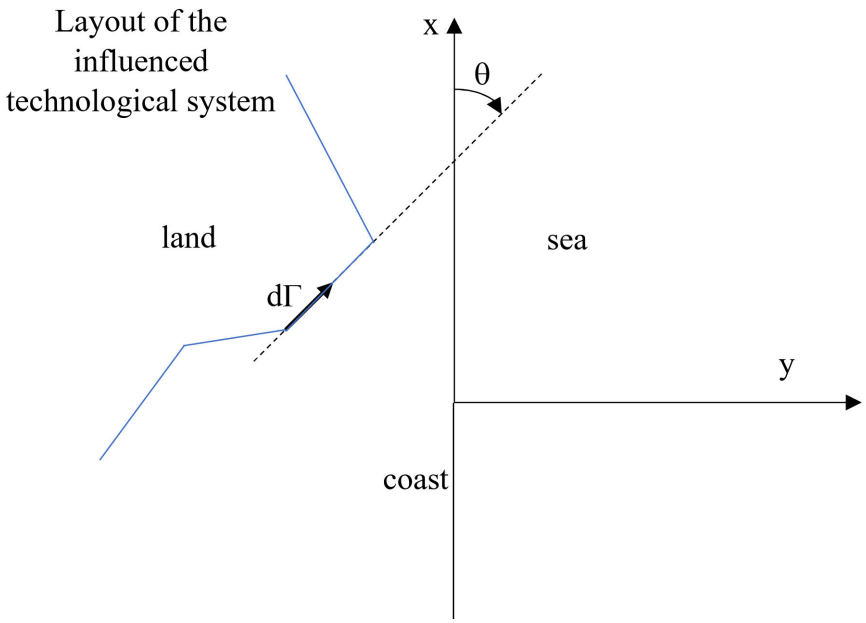

Figure 4. Definition of the orientation angle θ. This angle generally changes along the layout of the influenced technological system.

Since $d\vec{\Gamma}$ can be written as:

$$d\vec{\Gamma} = d\Gamma \cos\theta\, \vec{u}_x + d\Gamma \sin\theta\, \vec{u}_y \tag{11}$$

From equations (8), (10) and (11) we have:

$$\frac{de(y,f,\psi,\theta)}{d\Gamma} = e'(y,f,\psi,\theta) = E_x(y,f)(\cos\psi\cos\theta) + E_y(y,f)(-\sin\psi\sin\theta) \tag{12}$$

We may interpret the quantity e' as the component of the geoelectric field, having polarization defined by the angle ψ, along the direction defined by the angle θ.

This formula can be used in the step following the geoelectric field calculation i.e. the assessment of GIC and induced potential on the influenced infrastructure.

In fact, by representing the infrastructure by means of an equivalent transmission line circuit with ground return, the quantity *e'* plays the role of driving emf per unit length acting on the circuit itself (Wang et al., 2023; Lucca, 2024).

The solution of this equivalent circuit allows for the assessment of the GIC and induced potential on the infrastructure.

5. Example of application

We show an example of application by evaluating the geoelectric field in proximity of a coast of a shallow sea; we adopt a model of earth stratification by considering most of the data presented in (Chakraborty et. al. 2022; Boteler et al., 2023) and shown in Table 1.

Land side			Sea side		
description	***d* [km]**	**ρ [Ωm]**	**description**	***d* [km]**	**ρ [Ωm]**
sediments	0.1	10	seawater	0.1	0.3
crust	20	3000	crust	20	3000
mantle lithosphere	140	1000	mantle lithosphere	140	1000
upper mantle	247	100	upper mantle	247	100
transition zone	250	10	transition zone	250	10
lower mantle	∞	1	lower mantle	∞	1

Table 1. Earth stratification data

In the calculations, we have considered an incident geomagnetic field $H^0 = 1$ A/m.

In Fig. 5a, the geoelectric field is plotted as a function of the distance from the coast for different frequencies in case of H polarization

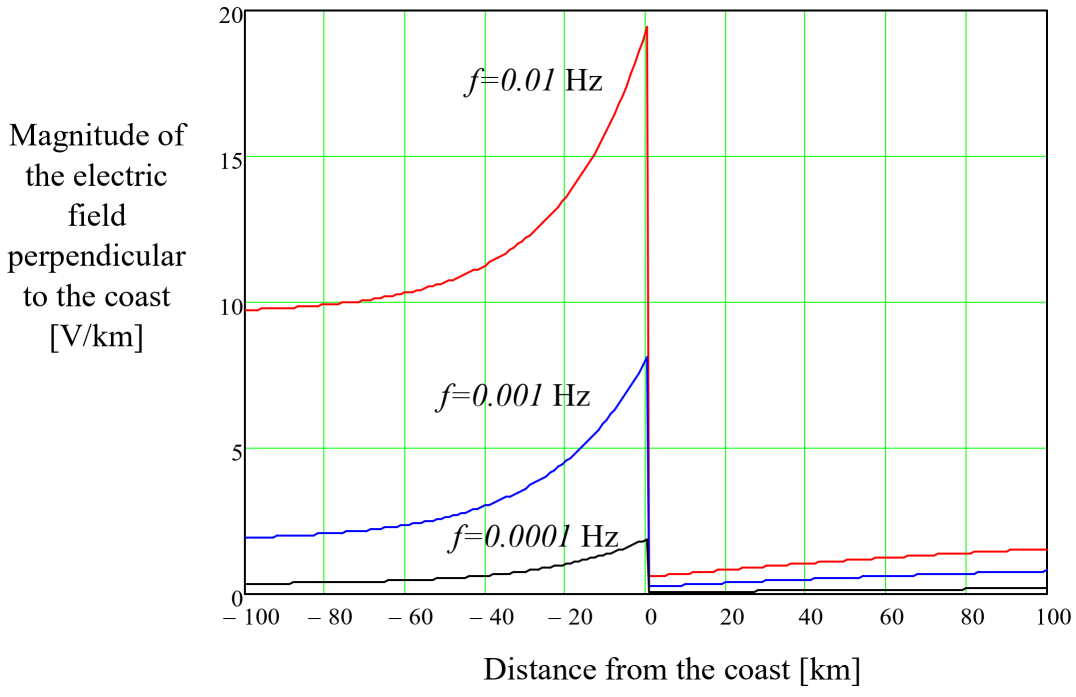

Figure 5a. Geoelectric field versus distance from the coast for different frequencies; H polarization.

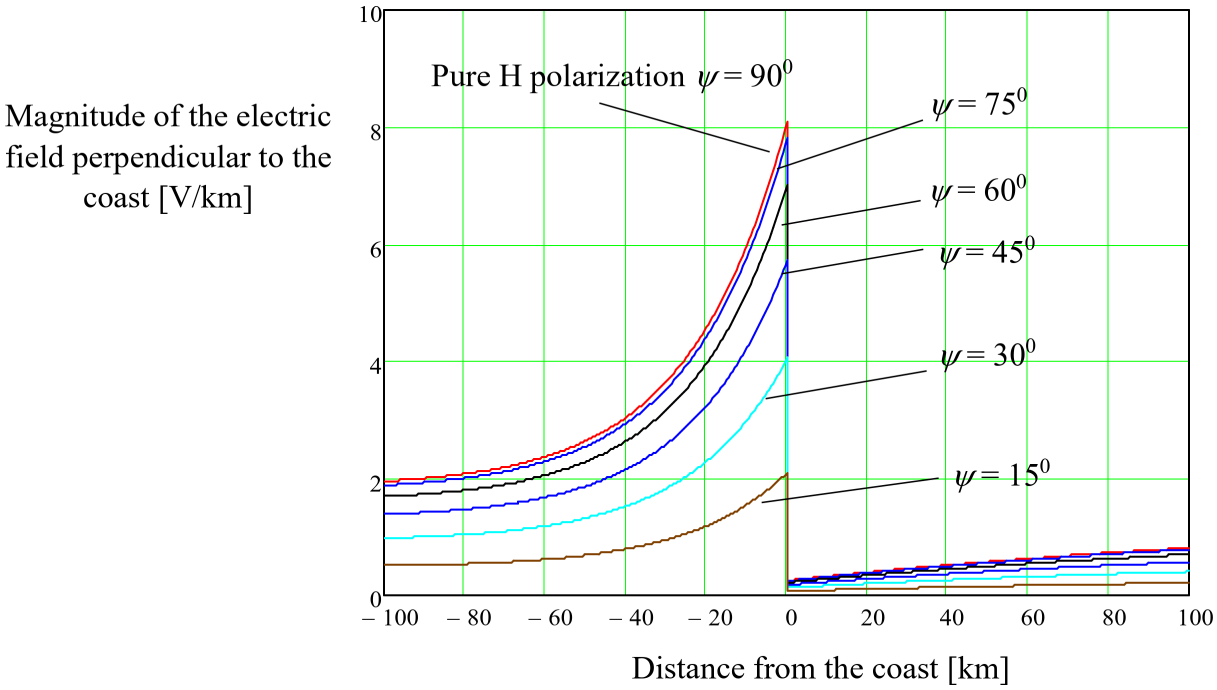

Figure 5b. y-component of the geoelectric field versus distance from the coast for different values of the polarization angle ψ; f = 0.001 Hz.

Figure 5a clearly shows the coast effect; in fact, at the coast itself the geoelectric field value is subjected to an abrupt change with respect to the one on the sea side; moreover, on the land side, it is considerably larger than the values it assumes several kilometers away from the discontinuity. This effect increases by increasing the frequency.

Figure 5b show the influence of the polarization angle ψ on the y component of the geoelectric field.

The main consequence of the coast effect is that a technological structure having its layout mainly perpendicular to the coastline is particularly exposed to the geoelectric induction; nevertheless, according to Fig. 5b, this effect is maximized when the polarization angle of the incident electromagnetic field is close to 90°.

By looking at Fig. 6a, we have examples of proximity effect for different values of frequency; in this case, in vicinity of the coast, and differently from the previous case, the field is decreased with respect to the value assumed far from the discontinuity. That is much more evident for the higher frequencies. Moreover, the geoelectric field, in this case, changes from the sea side to the land side without discontinuity and reaches its asymptotic value at a shorter distance from the coast.

Figure 6b show the influence of the polarization angle ψ on the x component of the geoelectric field.

The main consequence of the proximity effect is that a technological structure having its layout mainly parallel to the coast and not far from it, benefits from a reduction of the influencing geoelectric field; nevertheless, this effect is maximized when the polarization angle of the incident electromagnetic field is very close to 0°.

Let us consider now the case of a generic polarization. Figure 7a shows the modulus of the geoelectric field evaluated as a function of the polarization angle ψ for different distances from the coastline at the frequency of 0.001 Hz.

As expected, the geoelectric field presents the maxima for $\psi = 90°$ and $\psi = 270°$ that is when the incident wave is H polarized, while the minima appear when $\psi = 0°$ and $\psi = 180°$ that is when the incident wave is E polarized.

The amplitude of the field decreases by increasing the distance from the coast and, very far from it, the effect of the conductivity contrast between land and sea vanishes.

Fig. 7b shows the modulus of the geoelectric field versus the polarization angle ψ, evaluated at $y = 10$ km from the coastline but for different frequencies.

Also in this case, maxima and minima are found for $\psi = 90°, \psi = 270°$ and $\psi = 0°, \psi = 180°$ respectively; moreover, consistently with Figs. 5a and 6a the value of the field decreases by decreasing the frequency.

Figure 7c is a plot of the modulus of the geoelectric field versus the distance from the coastline for different values of the polarization angle ψ.

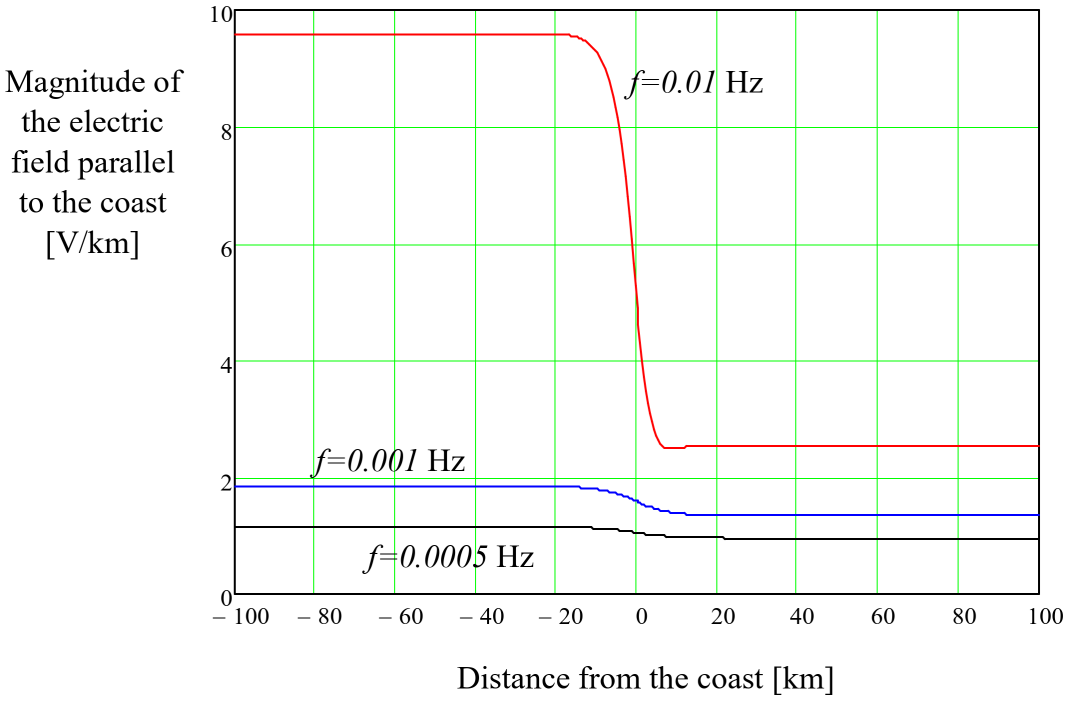

Figure 6a. Geoelectric field versus distance from the coast for different frequencies; E polarization.

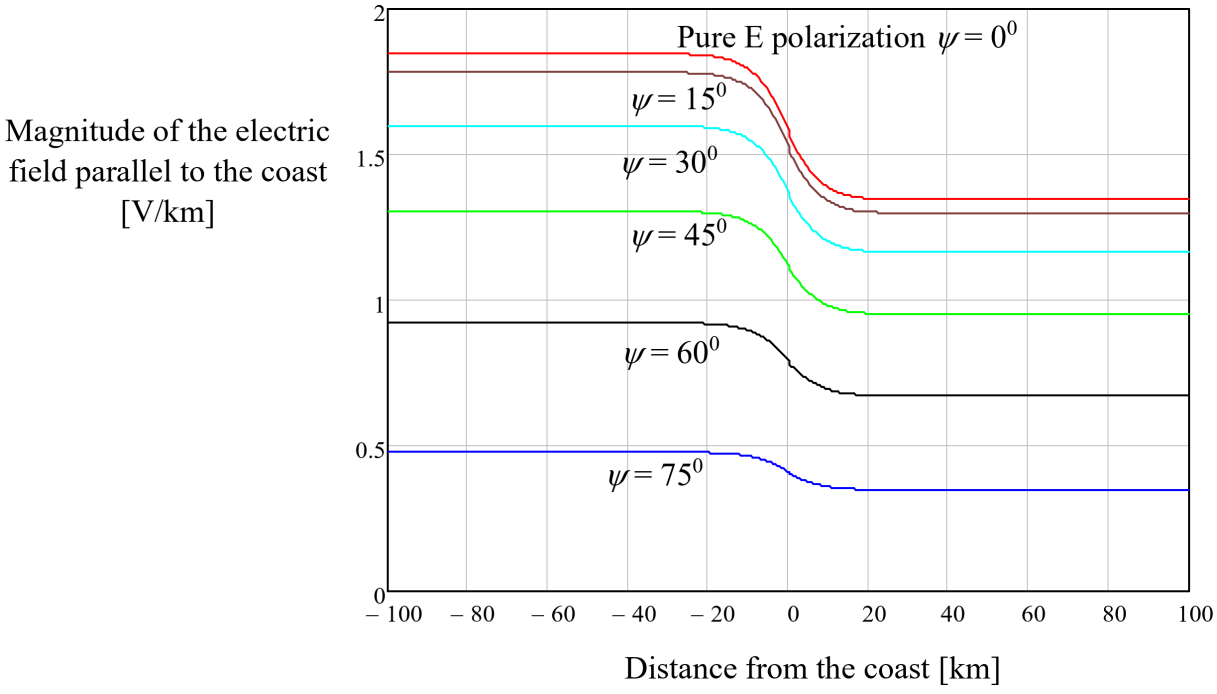

Figure 6b. x-component of the geoelectric field versus distance from the coast for different values of the polarization angle ψ; f = 0.001 Hz.

Figure 7c clearly points out the major weight of the H polarized component with respect to the E polarized component and this effect is evident also for small values of the polarization angle ψ.

Figures 8a, 8b and 8c show the contour plots of the quantity $e'(y, f, \psi, \theta)$, defined by means of Eq. (12), for a given frequency and a given distance from the coast as a function of the angles ψ and θ.

By looking at the contour plots of Figs. 8, one can notice that the maxima are corresponding to the pair of coordinates (ψ, θ) given by: (90°, 90°), (90°, 270°), (270°, 90°), (270°, 270°).

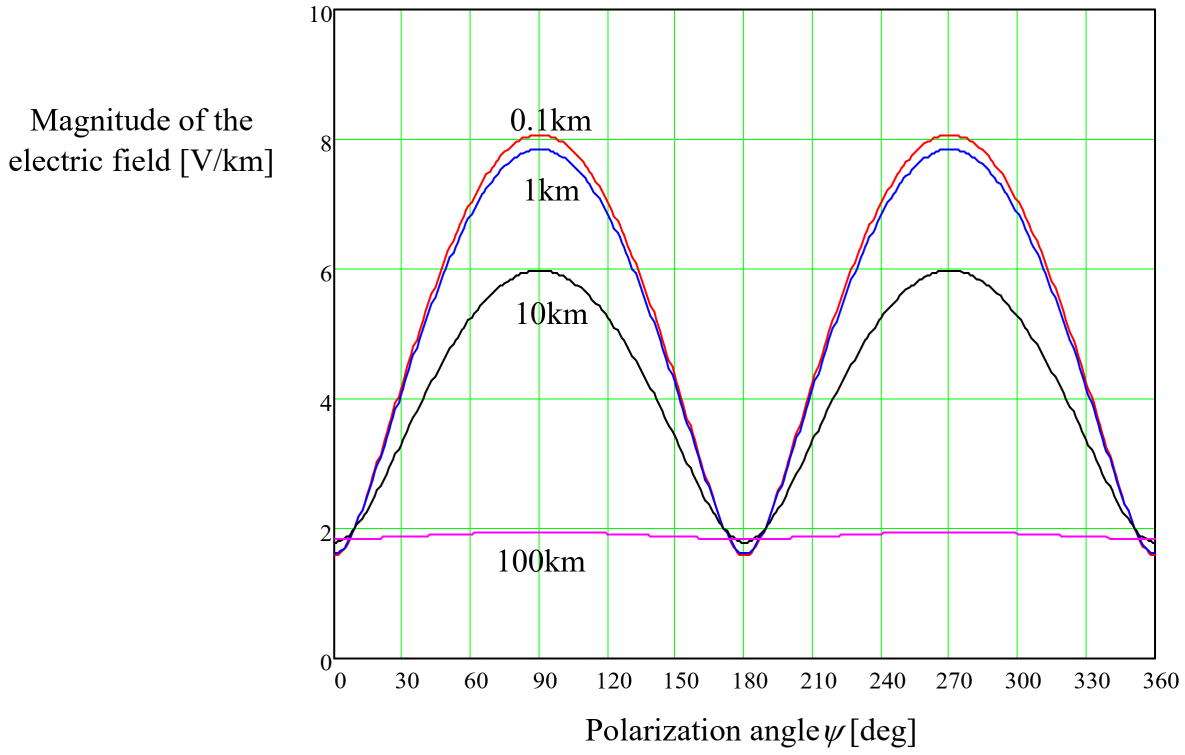

Figure 7a. Geoelectric field versus polarization angle at different distances from the coastline; $f = 0.001$ Hz.

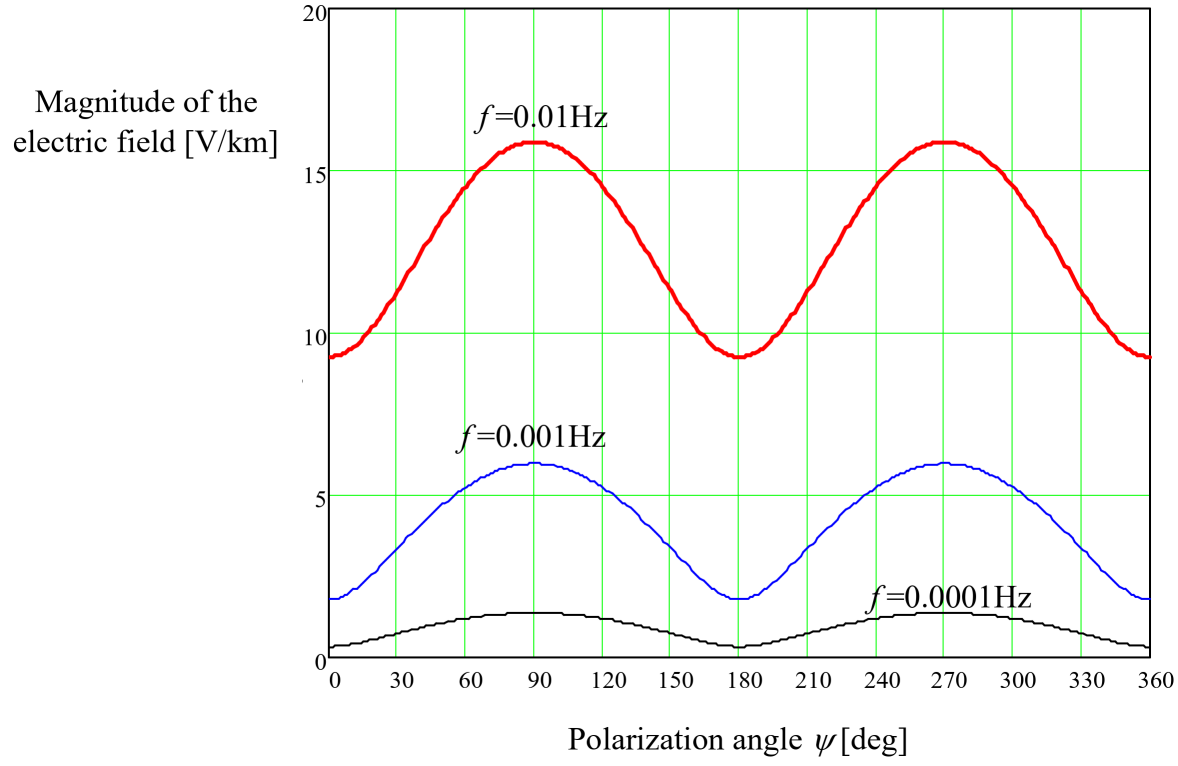

Figure 7b. Geoelectric field versus polarization angle at different frequencies; $y = 10$ km.

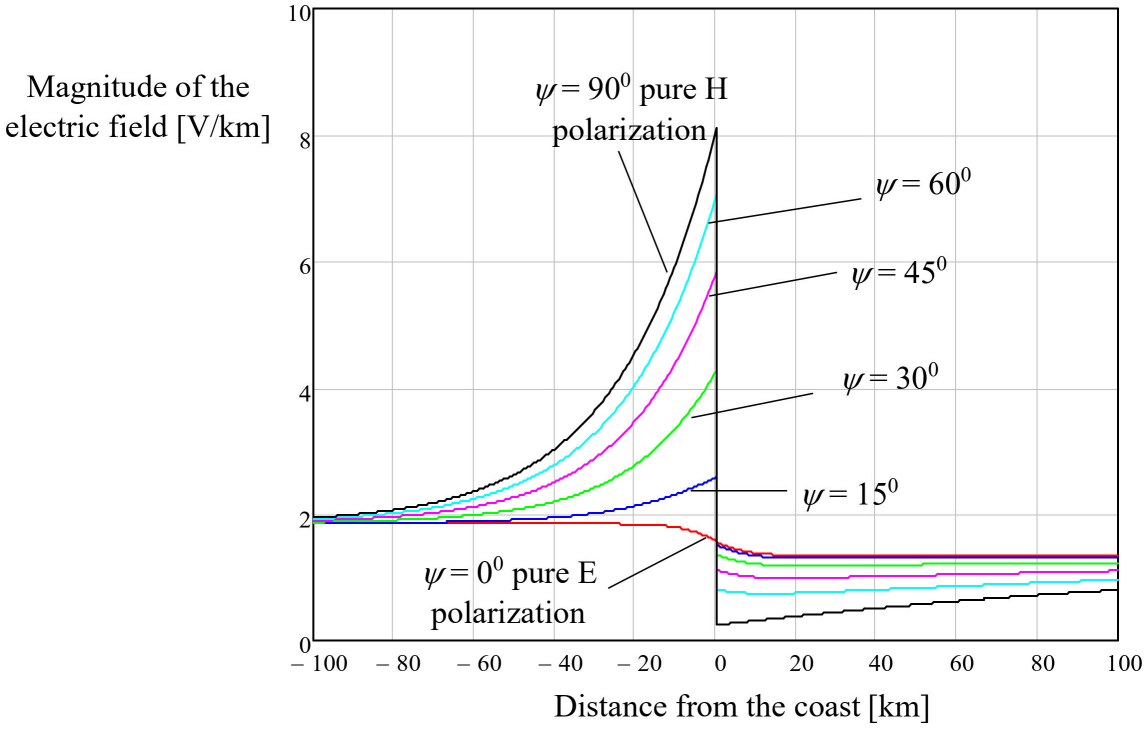

Figure 7c. Geoelectric field versus distance y from the coastline for different values of the polarization angle ψ; $f = 0.001$ Hz.

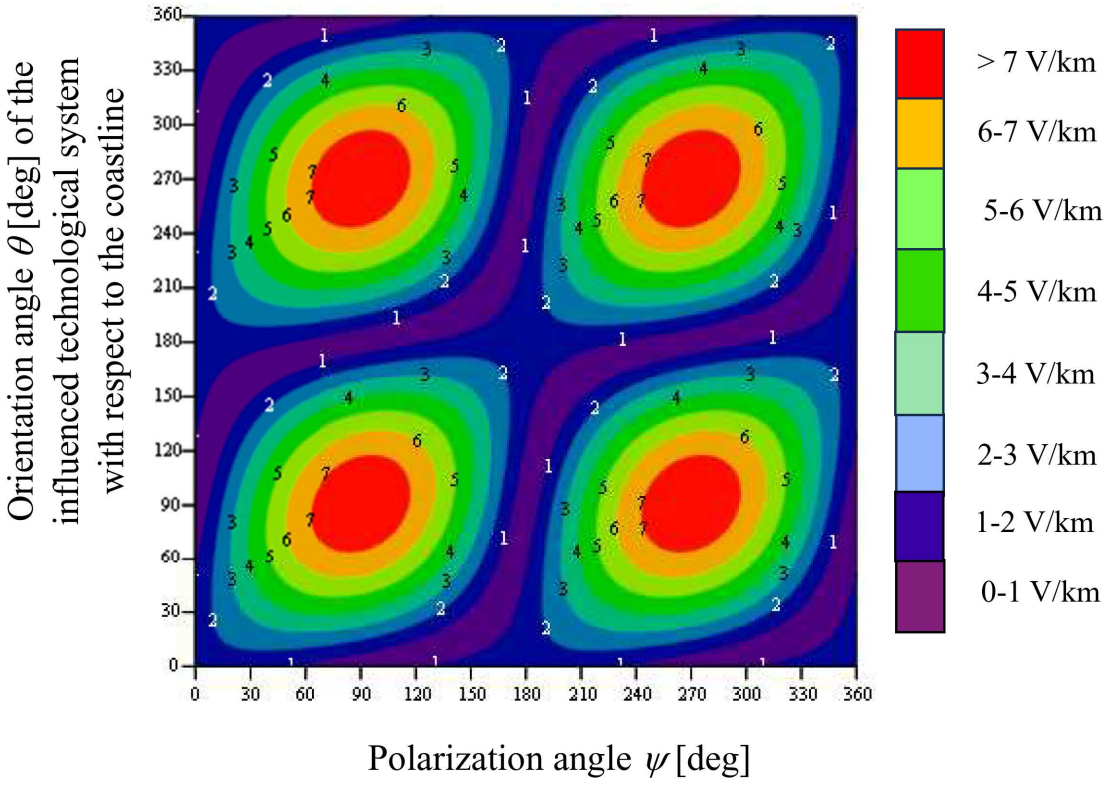

Figure 8a. Contour plots of e' (see Eq. (12)) in [V/km] for $y = 1$ km and $f = 0.001$ Hz; the numbers shown in correspondence of the contour plots represent the value of the geoelectric field component along the direction defined by the angle θ and having polarization given by the angle ψ.

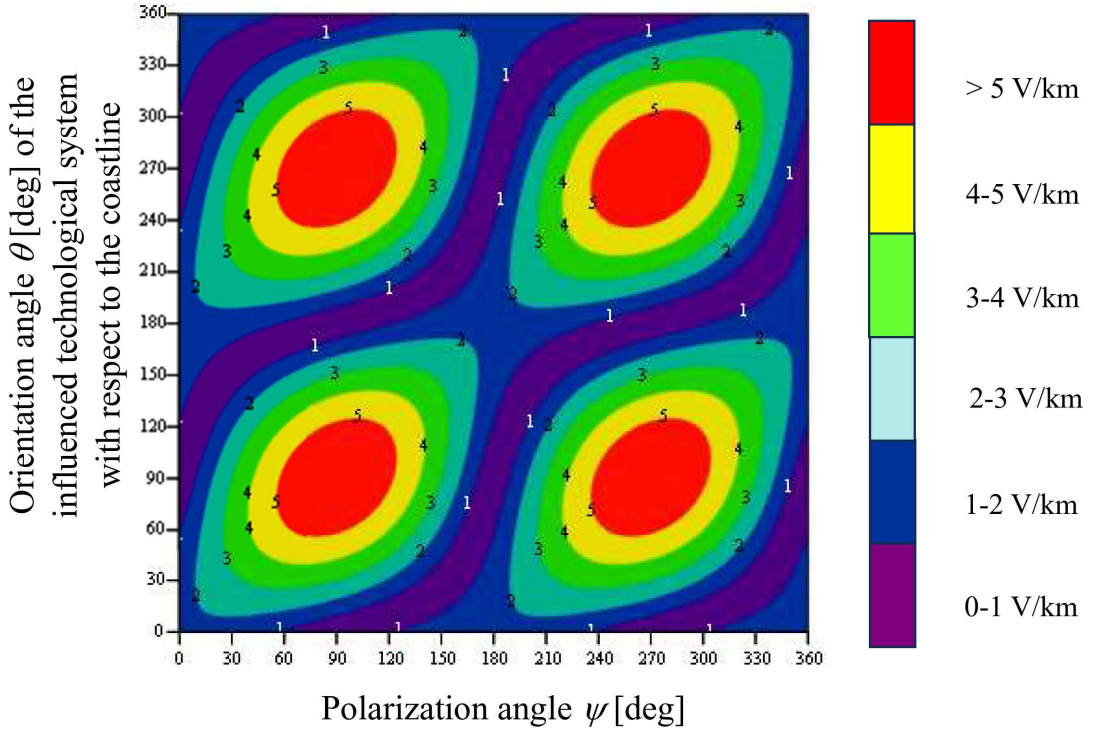

Figure 8b. Contour plots of e' (see Eq. (12)) in [V/km] for $y = 10$ km and $f = 0.001$ Hz; the numbers shown in correspondence of the contour plots represent the value of the geoelectric field component along the direction defined by the angle θ and having polarization given by the angle ψ.

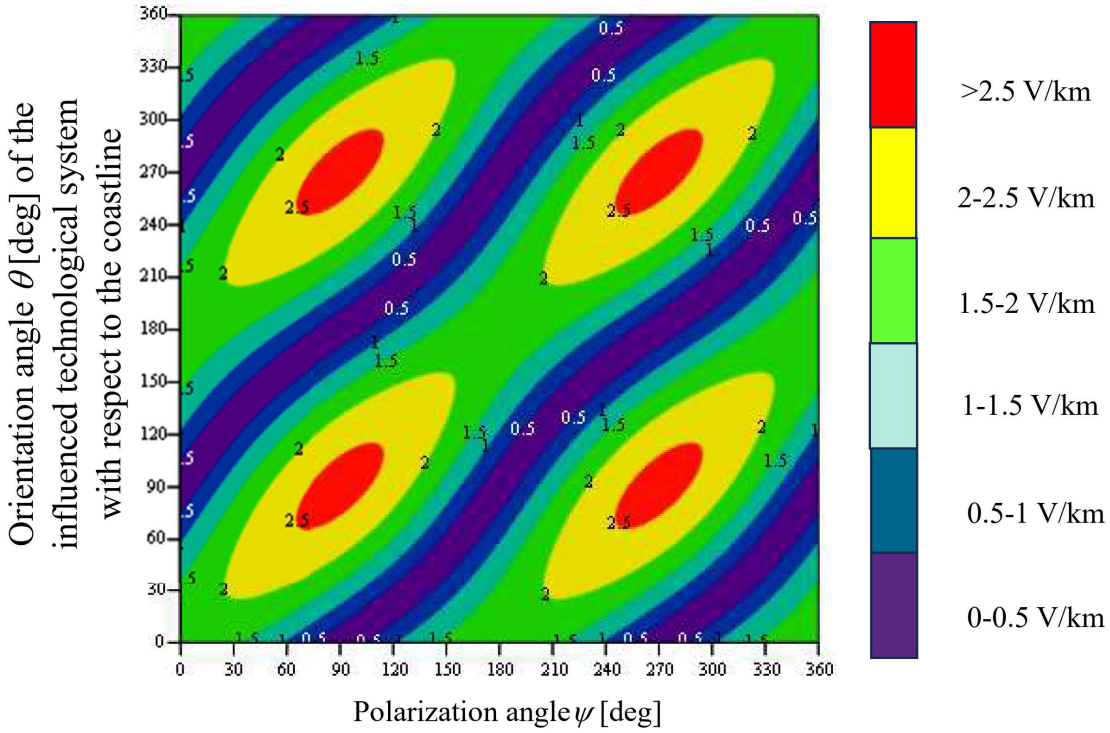

Figure 8c. Contour plots of e' (see Eq. (12)) in [V/km] for $y = 50$ km and $f = 0.001$ Hz; the numbers shown in correspondence of the contour plots represent the value of the geoelectric field component along the direction defined by the angle θ and having polarization given by the angle ψ.

For example, in Fig. 8a, the electric field is maximum for a polarization angle of 90° and in reverse direction i.e. perpendicular to the coast; then, a conductor will experience the maximum component of this electric field when it, too, is aligned perpendicular to the coast. The same can be noticed also in Figs. 8b and 8c even if the effect is attenuated due to the larger distance from the coast (10 km and 50 km respectively).

It can also be noticed that the contour plots get more elliptical by increasing the distance from the coast; this is due to a rebalancing of the relative weight between the component of the electric field, parallel to the coast, and the one perpendicular to the coast itself. This effect increases as the distance from the coast increases (see Fig. 7c).

In conclusion, also Fig. 8 confirm that, to have the maximum coupling with an influenced structure, its layout and the incident electric field must be both perpendicular to the coastline.

Hence, under these conditions we expect that GIC are maximized so resulting in the riskiest situation from the geomagnetic disturbance point of view.

6. Conclusions

In this paper, we have applied a 2D analytical model to a geoelectric induction problem aimed to evaluate GIC in technological infrastructures located near a coast.

The incident electromagnetic field is assumed to be in a generic polarization state that is expressed as a linear combination of E and H polarization; the calculation method of the geoelectric field is based on published formulas for H polarization while new analytical approximated formulas are proposed for E polarization and this represents the main novelty of the paper.

It is also known that when assessing the GIC in a technological infrastructure, an important role is also played by the directionality of its layout with respect to the coastline and, in relation to this point, thanks to the completely analytical formulation of the geoelectric field presented in this paper, we have also proposed a simple relationship, particularly tailored for calculation of GIC, as a function of the polarization angle ψ and of the angle θ expressing the orientation of the influenced infrastructure with respect to the coastline.

The application of the proposed method to some examples of calculation confirms what already mentioned in literature i.e.: the most critical case is when the incident wave is H polarized and the infrastructure layout is perpendicular to the coastline.

On the contrary, when the incident wave is E polarized and the infrastructure layout is parallel to the coastline, we have the most favorable case from the GIC point of view because the induced geoelectric field is reduced with respect to the value assumed far from the coast.

Objective of future work, will be the evaluation of GIC in technological infrastructure, located near a coastline, by applying the proposed calculation method with, possibly, comparison with measured data.

References

Ashour, A. A. (1973). Theoretical models for electromagnetic induction in the oceans, Phys. Earth Planet. Inter., 7, 303-312, doi:10.1016/0031-9201(73)90056-3.

Blake, J. R. (1968). The influence of coastal and sea floor geometry on natural electromagnetic variations of 10^{-4} to 10^{3} Hz, PhD Thesis, University of Alaska.

Boteler, D. H. (1999). Calculating the Voltages Induced in Technological Systems During a Geomagnetic Disturbance, IEEE Electromagn. Compat. Mag., 41, 398-402, doi:10.1109/15.809834.

Boteler, D. H. (2001a). Assessment of Geomagnetic Hazard to Power System in Canada, Nat. Hazards, 23, 101-120, doi:10.1023/A:1011194414259.

Boteler, D. H. (2001b). Geomagnetic hazards; in A Synthesis of Geological Hazards in Canada, (ed.) G. R. Brooks; Geological Survey of Canada, Bulletin 548, 183-206, doi:10.4095/212210.

Boteler, D. H. (2003). Geomagnetic Hazards to Conducting Networks, Nat. Hazards. 28, 537-561, doi:10.1023/A:1022902713136.

Boteler, D. H., S. Chakraborty, X. Shi, M. D. Hartinger et al. (2023). Transmission Line Modelling of Geomagnetic Induction in the Ocean/Earth Conductivity Structure, Int. J. Earth Sci., 14, 767-791, doi:10.4236/ijg.2023.148041.

Chakraborty, S., D. H. Boteler, X. Shi, B. S. Murphy et al. (2022). Modeling geomagnetic induction in submarine cables, Front. Phys., 10, 1-14, doi:10.3389/fphy.2022.1022475.

d'Erceville, I. and G. Kunetz (1962). The effect of a fault on the earth's natural electromagnetic field, Geophysics, 27, 651-665, doi:10.1190/1.1439075.

Dong, B., Z. Wang, R. Pirjola, C. Liu et al. (2015a). An Approach to Model Earth Conductivity Structures with Lateral Changes for Calculating Induced Currents and Geoelectric Fields during Geomagnetic Disturbances, Math. Probl. Eng., 2015, Article ID 761964, 1-10, doi:10.1155/2015/761964.

Dong, B., Z. Wang, L. Liu, L. Liu et al. (2015b). Proximity effect on the induced geoelectric field at the lateral interface of different conductivity structures during geomagnetic storms, Chin. J. Geophys., 58, 32-40, doi:10.1002/cjg2.20153.

Fischer, G. (1979). Electromagnetic Induction Effects at an Ocean Coast, Proceedings of the IEEE, 67, 1050-1060, doi:10.1109/PROC.1979.11388.

Gilbert, J. L. (2005). Modeling the effect of the ocean-land interface on induced electric fields during geomagnetic storms, Space Weather, 3, 04A03, 1-9, doi:10.1029/2004SW000120.

Liu, C., X. Wang, H. Wang and H. Zhao (2018). Quantitative influence of coast effect on geomagnetically induced currents in power grids: a case study, J. Space Weather Space Clim., 8, A60, 1-9, doi:10.1051/swsc/2018046.

Liu, C., X. Wang, C. Lin and J. Song (2019a). Proximity Effects of Lateral Conductivity Variations on Geomagnetically Induced Electric Fields, IEEE Access, 7, 6240-6248, doi:10.1109/ACCESS.2018.2889461.

Liu, C., X. Wang, S. Zhang and C. Xie (2019b). Effects of Lateral Conductivity Variations on Geomagnetically Induced Currents: H-Polarization, IEEE Access, 7, 6310-6318, doi:10.1109/ACCESS.2018.2889462.

Lucca, G. (2024). Geomagnetically induced potential on pipelines: A probabilistic approach, Adv. Space Res., 73, 3060-3068, doi:10.1016/j.asr.2023.12.043.

Pilipenko, V. A. (2021). Space weather impact on ground-based technological systems, J. Atmos. Sol.-Terr. Phys., 7, 68-104, doi:10.12737/stp-73202106.

Pokhrel, S., B. Nguyen, M. Rodriguez, E. Bernabeu et al. (2018). A Finite Difference Time Domain Investigation of Electric Field Enhancements Along Ocean-Continent Boundaries During Space Weather Events, J. Geophys. Res.: Space Phys., 123, 5033-5046, doi:10.1029/2017JA024648.

PRCI (Pipeline Research Council International) Report (2002). Telluric and Ocean Current Effects on Buried Pipelines and Their Cathodic Protection Systems, 14-17.

Price, A. T. (1949). The induction of electric currents in non-uniform thin sheets and shells, Q. J. Mech. Appl. Math., 2, 283-310, doi:10.1093/qjmam/2.3.283.

Ranganayaki, R. P. and T. R. Madden (1980). Generalized thin sheet analysis in magnetotellurics: an extension of Price's analysis, Geophys. J. Int., 60, 445-457, doi:10.1111/j.1365-246X.1980.tb04820.x.

Rankin, D. (1962). The magneto telluric effect on a dike, Geophysics, 27, 666-676, doi:10.1190/1.1439077.

Trichtchenko, L. and D. H. Boteler (2002). Modelling of geomagnetic induction in pipelines, Ann. Geophys., 20, 1063-1072, doi:10.5194/angeo-20-1063-2002.

Wang, X., D. H. Boteler and R. Pirjola (2023). Distributed-Source Transmission Line Theory for Modeling the Coast Effect on Geoelectric Fields, IEEE Transactions on Power Delivery, 38, 3541-3550, doi:10.1109/TPWRD.2023.3279462.

Wang, X. and S. Zhang (2023). The geoelectric field coast effect: Results from two dimensional finite element method and analytic solutions, Alex. Eng. J., 77, 525-536, doi:10.1016/j.aej.2023.06.089.

Weaver, J. T. (1963). The electromagnetic field within a discontinuous conductor with reference to geomagnetic micropulsations near a coastline, Can. J. Phys., 41, 484-495, doi:10.1139/p63-051.

Weaver, J. T. (1994). Mathematical Methods for Geo-electromagnetic Induction, Research Studies Press, Taunton, 111-112.

***CORRESPONDING AUTHOR: Giovanni LUCCA**,
Retired Indipendent Researcher, Piacenza, Italy
e-mail vanni.luccapc@gmail.com